Feng et al., J Gastroint Dig Syst 2017, 7:6
DOI: 10.4172/2161-069X.1000536

Journal of
Gastrointestinal & Digestive System

Research Article Open Access

Clinical analysis of CT and MRI Features of Solitary Fibrous Tumour of the Soft Tissues

Qian Yin Feng*, Surya Narayan Bayar, Mohammad Abdul Mazid, Deepak Bhandari, Li Xiao Hu and Li Hong Wen

Department of Radiology and Imaging, Anhui Medical University, China

Abstract

Objective: The aim of this study was to report and analyze outcomes associated twenty-eight patients' in-hospital evaluation of the computed tomography (CT) and magnetic resonance imaging (MRI) features of solitary fibrous tumors (SFTs) in various anatomic regions.

Methods: A number of twenty-eight patients whose clinical data, imaging finding, pathological and immune histochemical findings and with proven SFTs were retrospectively reviewed of the first affiliated hospital of Anhui medical university of January 2012 to 2015 were identified and included for analysis. Twenty-one patients (17 with contrast) had undergone CT scan while 7 (4 with contrast) had undergone MRI. Image characteristics and pattern of enhancement on CT and MRI were analyzed and compared with histopathological findings and multivariate analysis.

Results: Among 28 patients, 12 SFTs occurred in the thoracic cavity, 4 in the mediastinum, 3 in the retro-peritoneum, 2 in the meanings while a single SFT was found in other 7 organs. They appeared as a solitary mass with an oval or irregular shape, well-defined or ill-defined margin. The size ranged from 1.5 ×1.0 cm^2 to 23.0 × 16.5 cm^2. Plain CT revealed homogeneous iso-density in 10 and heterogeneous iso-density in 11 cases. Out of the 17 contrast enhanced cases, 11 cases showed slight enhancement and 6 showed marked heterogeneous enhancements during the arterial phase (AP). Progressive and prolonged enhancement was observed in the dynamic contrasted scan. Most of tumors (14/17) exhibited serpentine vessel sign in AP. Hypo- or iso-intensity on T1WI and hyper-or iso-intensity onT2WI were revealed on MRI. Six cases (6/7) showed the flow voids sign on T2WI.

Conclusion: SFTs typically present as large, well-defined, heterogeneous, progressively enhancing mass in pleural and extra-pleural regions. The valuable diagnostic features are serpentine vessels in arterial phase (CT) and flow voids sign on T2WI (MRI).

Keywords: Solitary fibrous tumor; Soft tissue; Computed tomography; Magnetic resonance imaging

Introduction

Tumors originating from mesenchymal tissues are rarely encountered in radiology clinics. Among them, Solitary fibrous tumor (SFTs) is the rarest form of spindle cells tumor which was firstly described by E. Wagener during the 1870's. These tumors can be present anywhere in the body where muscle tissue exist however the first case report was described in pleura [1]. With time, these SFT's were noticed at different locations like - head and neck regions such as cheek, orbit, oral cavity, laryngeal and para-pharyngeal space retro-peritoneum, abdomen and pelvis and the soft tissues of the extremities [2-11]. These tumors have been classified as intermediate malignancies that rarely metastasize by the World Health Organization in 2002. The tumor is typically composed of spindle cells surrounded by dense collagenous stroma, which usually contain hyper- and hypo-cellular areas [12]. Moreover, studies on pleural samples too have demonstrated its benign nature with only approximately 10% recurring locally or metastasizing [13-15].

The common and gold standard for diagnosing SFT's so far, has been direct histological observation that exhibits variable pleomorphic spindle cells mixed with collagen arranged randomly and the immune histochemical staining of tumor markers like- CD34, Vimentin and bcl-2 are almost always positive [16]. However, these tumors are silent in nature, smaller in size, variably located and easily mistaken with other commonly occurring neoplasm such as angio-sarcoma, lipo-sarcoma, adenolymphoma, schwannoma, hemangioma etc. With these varieties of differentials, patients with SFT's are initially subjected to imaging modalities before clinician advices for histological studies. Keeping this fact in mind, radiological scholars for the last decade have put in an enormous effort at diagnosing these SFT's by means of imaging techniques. Radiologists have been able to diagnose this tumor by means of CT that can accurately determine its size, morphology, location and topography while MRI, USG, PET have been helpful too but less used.

Similarly, SFT being a rare disease, we find limited number of research articles and most of these, center around case presentations and case discussions. We, too, are presenting the cases of SFT observed at our center. We have conducted a retrospective study of 28 cases of histologically proven SFT exploring the radiological features observed. By doing so, we validate the radiological diagnosis of these benign tumors based parallel with histology. This we expect would further reinforce the imaging modality for diagnosing SFT, a clinical need at times of early diagnosis and early institution of treatment, where time-clock ticks. We also feel that a larger trial is necessary to validate the findings of this study as it would address other issues, not addressed by a retrospective study.

***Corresponding author:** Qian Yin Feng, Department of Radiology and Imaging, Anhui Medical University, China, Tel: +86-13866187805; E-mail: 894206876@qq.com

Received November 25, 2016; **Accepted** November 20, 2017; **Published** November 27, 2017

Citation: Feng QY, Bayar SN, Mazid MA, Bhandari D, Hu LX, et al. (2017) Clinical analysis of CT and MRI Features of Solitary Fibrous Tumour of the Soft Tissues. J Gastroint Dig Syst 7: 536. doi: 10.4172/2161-069X.1000536

Methods

Source

The hospital database and medical records were explored, tabulated and tallied. There were 28 patients that had been histologically diagnosed with SFTs from 2012 to 2015. The clinical data, imaging findings, pathological and immune histochemical findings were retrospectively analyzed.

Scan technique

Out of the total, 21 patients were scanned using a 64-slice MDCT scanner (GE light speed, VCT, American), 17 of them underwent contrast enhanced scan. The scanning parameters were as follows: tube voltage, 120 kVp; tube current, 400 mA; the helical scan with pitch ratio, 1.375:1; collimation thickness, 0.625 mm × 64 and the slice thickness, 5 mm. The contrast enhanced scan was performed using 100 ml intravenous contrast material (Omnipaque 300; Amersham Health, Princeton, NJ). The scanning time for contrast-enhanced scan was as follows: neck, 25 s, 40 s was delayed after injection; chest, 40 s was delayed after injection; abdominal regions, 30, 60, 120 s were delayed for arterial, portal and venous phase (AP, PP, VP) scanning. The contrast agent was injected at a rate of 3 mL/sec.

Seven patients of the total were scanned using a 3.0 T MRI unit (GE, SignaHDxt, America). Four of them underwent contrast enhanced scan. The scanning parameters were: a T1WI FSE sequence (TR720 ~ 1972 ms, TE12.0 ~ 21.9 ms) and FSE sequence T2WI (TR4480 ~ 8571 ms, TE95.0 ~ 119.6 ms), a contrast enhanced imaging was obtained with T1WI LAVA (TR 2.6, 1.2) or 3D BRAVO (TR 7.8, TE3.0), by the Gd-DTPA were injected at a rate of 2 ~ 3 mL/s. Moreover, one patient underwent both CT scan as well as MR scan, with same parameters.

Image analysis

The CT and MRI images were reviewed by 2 radiologists with 5 year experience of radiology diagnosis in consensus. For each lesion, the features of location, size, margin, shape, density (CT), signal intensity (MRI), enhancement pattern, vessel sign, flow voids and infiltration to adjacent tissues were analyzed. The density of the lesion was evaluated as homogeneous or heterogeneous on the plain scan and the exact CT value was measured. The pattern of enhancement was graded as slight, moderate, marked homogeneous or heterogeneous. The CT value of solid component of each phase was measured. The vessel sign of the tumor was reviewed in AP (CT) and the flow voids sign in the T2WI (MRI).

Results

Clinical data

The tumor occurred between the ages of 25-78 years with a mean age falling in the 5th decade. There were 17 females and 11 males. Of the 28 patients, 11 (40%) patients were asymptomatic, found by incidental CT or MRI examination. 2 patients (7.1%) presented chest pain and chest tightness, 4 (14.2%) patients complained of irritable cough and other 4 (14.2%) patients with palpable mass during physical examination, Abdominal pain in 2 (7.1%) patients and each 1 (3.5%) patient with loss of consciousness with hyperspasmia, neck pain, nasal obstruction respectively. The specific proportions of distribution of symptoms are depicted in Figure 1.

Imaging findings

Tumor location was formulated in Figure 2. Twenty-eight lesions were found in different regions such as the thoracic cavity (n=12), mediastinum (n=4), retro-peritoneum (n=3), parotid gland (n=1), adrenal gland (n=1), kidney (n=1), para-pharyngeal space (n=1), abdominal cavity (n=1), nasal cavity (n=1), meninges (n=2), cervical spinal canal (n=1) (Figure 2).

All the CT and MRI findings are presented in Tables 1 and 2. The

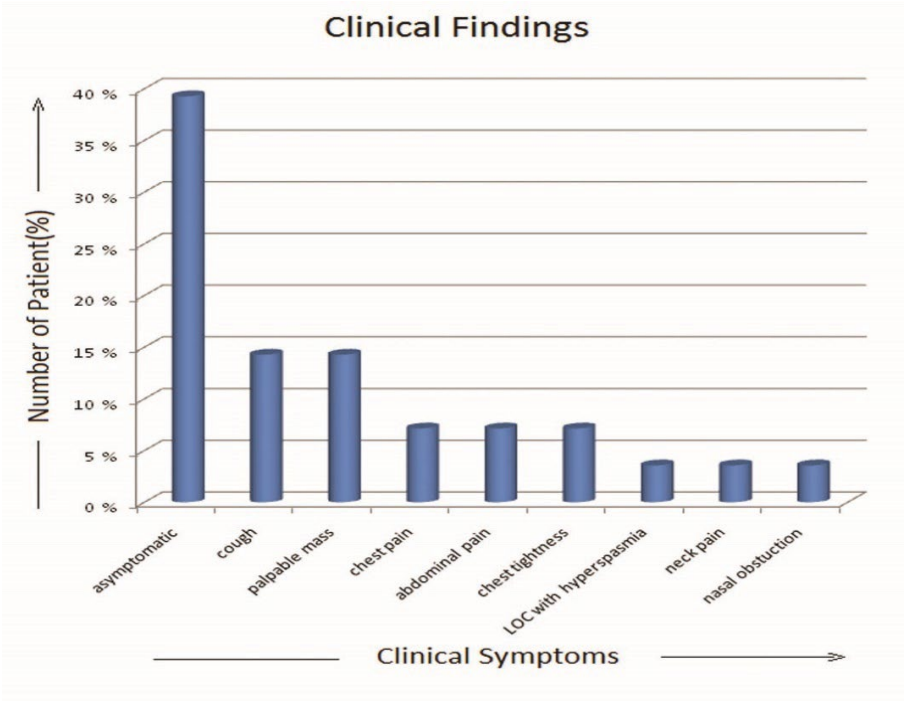

Figure 1: The specific proportions of distribution of symptoms.

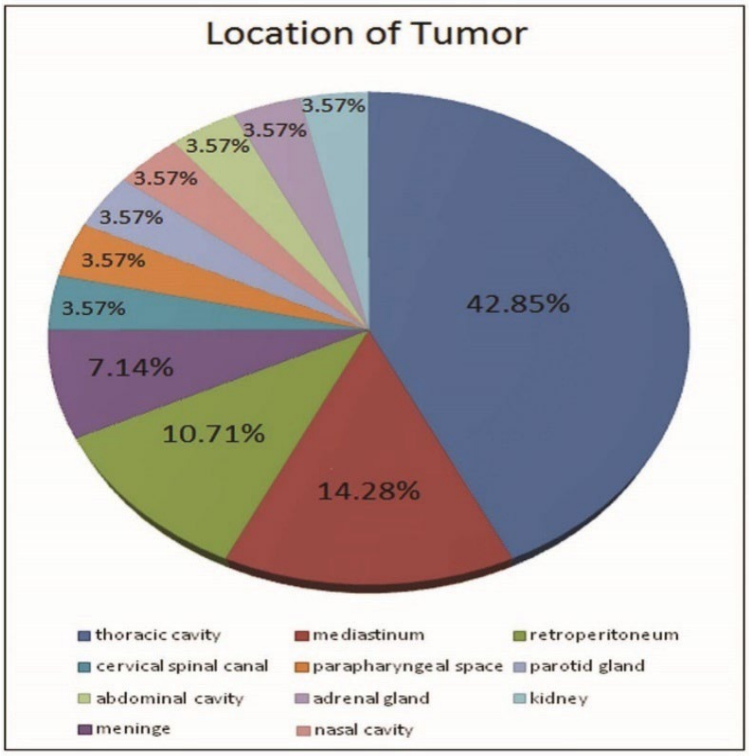

Figure 2: Locations of tumor.

Case	Location	Size (cm²)	Shape/Margin	Density/Cystic Changes	Enhancement Pattern	Vessel sign	Infiltrative Manifestation	Previous Diagnosis	Nature	Rec.
1	Thoracic cavity	9.0 × 8.2	Oval/Well-defined	Homo/-	Slight, Hetero	+	-	Mesothelioma	B	-
2	Thoracic cavity	10.0 × 7.2	Irreg/Well-defined	Homo/-	/	/	-	Mesothelioma	B	-
3	Thoracic cavity	17.2 × 14.5	Irreg/Well-defined	Hetero /+	Slight, Hetero	+	Pericardial and Pleural effusion	Sarcoma	B	-
4	Thoracic cavity	6.7 × 4.8	Irreg/Ill-defined	Hetero /-	/	/	Invasion to Pericardium	Sarcoma	M	+
5	Thoracic cavity	10.3 × 8.0	Irreg/Well-defined	Homo /-	Slight, Hetero	+	-	SFT	B	-
6	Thoracic cavity	6.3 × 6.0	Oval/Well-defined	Hetero /+	Slight, Hetero	+	-	Mesothelioma	B	-
7	Thoracic cavity	12.7 × 11.0	Oval/Well-defined	Homo /-	Slight, Hetero	+	Pleural effusion	Sarcoma	B	-
8	Thoracic cavity	8.0 × 7.1	Irreg/Ill-defined	Homo /+	Marked,Hetero	-	-	Thymoma	B	-
9	Thoracic cavity	11.0 × 12.4	Oval/Well-defined	Hetero /+	/	/	Pleural effusion	Leiomayosarcoma	B	-
10	Mediastinum	8.5 × 7.0	Oval/Well-defined	Hetero /+	Slight, Hetero	-	Pericardial effusion	Schwannoma	M	+
11	Mediastinum	23.0 × 16.5	Oval/Well-defined	Hetero /+	Slight, Hetero	+	Pericardial effusion	SFT	B/M	-
12	Mediastinum	5.5 × 5.4	Oval/Well-defined	Homo /-	Marked,Hetero	+	-	Lymphoma	M	+
13	Nasal cavity	2.0 × 1.7	Oval/Well-defined	Homo /-	/	/	-	Fibroma	B	-
14	Parotid gland	4.8 × 3.0	Irreg/Ill-defined	Homo /-	Marked,Hetero	+	Invasion to Parapharyngeal Space	Nasopharyngeal Angiofibroma	M	-
15	Lt.Parapharyngeal space	5.8 × 5.0	Irreg/Ill-defined	Hetero /-	Marked,Hetero	+	Invasion to Parapharyngeal Space	Nasopharyngeal Ca	B	-
16	Adrenal gland	8.5 × 7.0	Oval/Well-defined	Homo /-	Slight, Hetero	-	-	Adrenal Adenoma	B	-
17	Abdominal cavity	6.8 × 5.0	Oval/Well-defined	Homo /-	Marked,Hetero	+	-	Castleman disease	B/M	-
18	Lt. Kidney	15.0 × 12.7	Oval/Well-defined	Hetero /+	Slight, Hetero	+	-	Renal Ca	B	-
19	Retroperitonium	11.0 × 10.3	Oval/Ill-defined	Hetero /+	Slight, Hetero	+	-	Sarcoma	B	-
20	Retroperitonium	19.8 × 17.5	Irreg/Well-defined	Hetero /-	Slight, Hetero	+	-	Lyposarcoma	B/M	-
21	Retroperitonium	11.0 × 10.4	Oval/Well-defined	Hetero /-	Marked,Hetero	+	-	Hemangiopericytoma	B	-

Table 1: CT findings of 21 patients; [Homo: Homogeneous, Hetero: Heterogeneous, B: Benign, M: Malignant, B/M: Borderline, '+' positive, '-' negative, Ca: carcinoma, CT: Computed tomography, irreg: Irregular, '/' not done, Rec: Recurrence, Lt.: Left].

tumor size ranged from 1.5 × 1.0 cm² to 23.0 × 16.5 cm², with an average size of 9.4 × 7.6 cm². We found two cases with small size (2.0 ×1.7 cm² and 1.5 ×1.0 cm²) occurred in the nasal cavity and the cervical spinal canal respectively due to their early symptoms. Eighteen lesions (18/28) had an oval shape and 10 (10/18) had an irregular shape, with well-defined margin in 23 and ill-defined margin in 5 lesions.

On CT images, these tumors appeared homogeneous in 10 cases (10/21) and heterogeneous in 11 (11/21) cases with an average CT of

Case	Location	Size(cm2)	Shape	Flow voids sign	T1WI	T2WI	Enhancement pattern	Infiltrative manifestation	Previous diagnosis	Nature	Rec.
1	Thoracic cavity	15.6 ×13.0	Oval/Well-defined	+	Hypo	Hyper	Slight, Hetero	Pleural effusion	Sarcoma	B/M	-
2	Thoracic cavity	3.5 × 3.2	Oval/Well-defined	+	Iso	Mild-hyper	Marked, Homo	-	Mesothelioma	B	-
3	Thoracic cavity	11.6 ×10.0	Irreg/Well-defined	+	Iso	Mild-hyper	/	-	Mesothelioma	B	-
4	Meninges	6.0×5.5	Oval/Well-defined	+	Hypo and iso	Hyper and iso	Slight, Hetero	-	Schwannoma	B/M	-
5	Meninges	4.4×3.4	Irreg/Well-defined	+	Iso	Iso	Marked, Homo	-	Meningioma	B/M	-
6	Mediastinum	7.7×6.7	Oval/Well-defined	+	Hyper	Hyper	/	-	Mediastinum-type lung Ca	B/M	-
7	Cervical Spinal Canal	1.5× 1.0	Oval/Well-defined	-	Iso	Mild hyper	/	-	Fibroma	B	-

Table 2: MRI findings of 7 patients; [iso: isointense, hypo: hypo-intense, hyper: hyper-intense, B: benign, M: malignant, B/M: borderline malignant, '+' positive, '-' negative, MRI: Magnetic Resonance Imaging, T1WI: T1 Weighted Imaging, T2WI: T2 Weighted Imaging, irreg: irregular, '/' not done, Rec: recurrence].

Case	CD-34	Vimentin	CD 99	Bcl-2	S-100	SMA	CK	Desmin	CD117	KI-67	EMA	Nature
1	+	+	+	+	-	-	-	-	-	-	-	B
2	+	+	+	+	-	+	-	-	-	+	-	B
3	+/-	+	+	+	-	+	-	-	-	+	+	M
4	+	-	+	+	-	-	-	-	-	+	-	B
5	+	+	+	+	+	-	-	-	-	+	-	B
6	-	+	+	+	+	-	-	-	-	+	-	B/M
7	+	+	-	+	-	-	-	-	-	10%	-	B
8	+	+	+	+	-	+	-	-	+/-	5%	-	B/M
9	+	+	+	+	+	-	-	-	-	8%	-	M
10	+	-	+	+	-	-	-	-	+	30%	+	B
11	+	+	+	+	-	-	-	-	-	1%+	-	B
12	-	+	+	+	-	+	-	-	-	+	-	B
13	-	+	+	+	-	-	-	-	-	<1%	-	B/M
14	+	-	+	+	-	-	-	-	-	1%+	-	B
15	+	+	+	+	-	-	-	-	-	+	-	M
16	+	+	+	+	+	-	-	-	-	20%+	-	B/M
17	+	+	+	+/-	-	-	-	+	-	10%+	-	B
18	+	+	+	+	-	-	-	-	-	4%+	-	B
19	+	+	+	+	-	-	-	-	-	2%+	-	B
20	+	+	-	+	-	+	-	-	-	3%+	+/-	B
21	+	+	+	+	-	-	-	-	-	8%+	-	B
22	+	+	+	+	-	-	-	-	-	3%+	-	B
23	+	+	+	+	-	-	-	-	-	3%+	-	B
24	+	+	+	+	-	+	-	+	-	8%+	-	B
25	+	+	+	+	-	-	-	-	-	1%+	-	B
26	+	+	+	+	-	-	-	-	-	4%+	-	B
27	+	+	+	+	-	-	-	-	-	7%+	-	B
28	+	+	+	+	-	-	-	-	-	4%+	-	B

Table 3: The immune histochemical results of 28 patients; ['+' Positive, '-' Negative, '+-' Partial positive, 'B': Benign, 'M': Malignant, 'B/M': Borderline malignant].

the solid component being 41.5 HU. Among the 17 cases that received radio-contrast, 11 of them showed slight enhancement and 6 showed marked heterogeneous enhancements during the arterial phase. During the 8 cases with dynamic CT scan, 6 cases in the abdominal region showed slight and progressive enhancement and the average CT value in AP, PP, VP was respectively 46.4, 73.3, 86.5 HU. Two cases in neck region displayed marked enhanced in AP and persistent in VP, with 165 HU in AP and 186 HU in VP. Fourteen cases (14/17) presented positive vessel sign. Additionally, the CT scan also demonstrated cystic changes within the tumor in 9 cases. On MRI images, most of the tumors were homogeneous hypo or iso-intense on T1WI and heterogeneous hyper or iso-intense on T2WI. Of the 4 contrasted cases, 2 cases were observed marked homogenously enhanced and 2 were slight heterogeneously enhanced. Six cases (6/7) presented flow voids sign on T2WI. Nine (9/28) tumors were observed infiltrative to adjacent tissues, most cases with pleural and pericardial effusion seen in thoracic cavity and mediastinum.

Pathological findings

All of the 28 patients had undergone surgical excision and a solitary mass was found. All of the 28 lesions were resected completely and proven SFT by histopathological and immune-histochemical analysis. Most tumors were found oval shape with intact capsule. These tumors were composed of hyper and hypo cellular spindle cells with proliferation and surrounded by collagen fibers. The cut sections of these tumors had a grayish white or yellowish white color with a

fish-meat like texture. Besides these features, some of the lesions also demonstrated irregular areas of myxoid degeneration and necrosis with internal hemorrhage. Immunological staining was strongly positive for CD 34, Vimentin, Bcl-2, while negative for SMA, CK, the details are summarized in Table 3. Of the 28 lesions, 21 were proven benign, 3 were malignant and 4 were borderline nature. Three patients with the tumor located in the thoracic cavity and mediastinum had recurrence after surgery during a 36 months follow up period.

Discussion

The SFT is an uncommon spindle cell tumor of mesenchymal origin with age onset of around 50-60 years and equal distribution in male and female. Patients in our study ranged from 26-78 years, found approximately equally in female (60%) and male (40%). Most commonly SFT arises from the visceral or parietal pleura but can also occur in extra-pleural region. In this study, we reported the tumors occurred in pleural and various extra-pleural regions such as retro-peritonium, abdominal cavity, meninges, nasal cavity, para-pharyngeal space, parotid gland and cervical spinal canal. Clinically SFT usually presents as a slow-growing, asymptomatic mass incidentally found by imaging examination during general check-up. Patients with pleural SFT usually present chest pain or distress symptoms. Compression symptoms or a palpable mass usually occurred in patients due to a large size of tumor. The final diagnosis of SFT depends on the histopathological and immune-histochemical analysis. The tumor is typically composed of spindle cells surrounded by dense collagenous stroma, which usually contains hyper- and hypo-cellular areas [12]. Areas of hyalinization, necrosis and myxomatous degeneration are occurred more frequently in larger lesions [17-19]. The immune-histochemical reaction is the key to differentiate SFT with others spindle cell tumor. It almost presents positive expression for CD 34, bcl-2, vimentin and negative expression for S100, SMA. CD 34 is defined as a highly specific marker for this tumor [16].

Morphologically, SFT mostly presents as a well-defined oval shape tumor with different sizes. Smaller size generally occurs in the subcutaneous or superficial organs and larger size occurs in deep tissue such as the chest cavity, abdominal cavity and retro-peritoneum. We found two cases with small size (2.0×1.7 cm^2 and 1.5×1.0 cm^2) occurred in the nasal cavity and the cervical spinal canal respectively due to their early symptoms.

On CT images, the density on plain scan is related to the pathological component of the tumor. Plain scan can reveal small SFT as homogeneous iso-dense solid lesions while larger lesions are mostly heterogeneous with patchy low density. On contrasted images, the enhancement pattern and degree also depend upon the tumor components and proportion of spindle cells, vessels and collagen fibers. Obvious marked enhancement is related to hyper-vascular and hyper-cellular areas, while hypo-cellular and collagen-rich areas showing slight enhancement [18]. Areas of myxomatous degeneration or necrosis usually present as lower density or cystic changes with no enhancement inside the tumor [20]. In accordance with the aforementioned facts, we induced two types of enhancement pattern found in our cases. One pattern is moderate or marked homogenous or heterogeneous enhancement on AP and persistent enhancement on delayed phase, correlated with hyper-cellular and vascular component. Another is slight enhancement on AP and progressive enhancement on delayed phase, correlated with hypo-cellular and rich collagenous component in the tumor. In this group, all of the 6 cases in the abdominal region presented slight enhancement in AP and gradually enhanced in PP and VP (Figure 3). Two of our cases in the neck region presented marked enhancement in AP and persistent enhancement in VP (Figure 4). While only 8 of our 17 enhanced cases have taken the dynamic scan, which is the limitation of this study. But our findings are corresponding with previously reported study which also revealed this enhancement feature [17]. Due to the hyper-vascular feature of

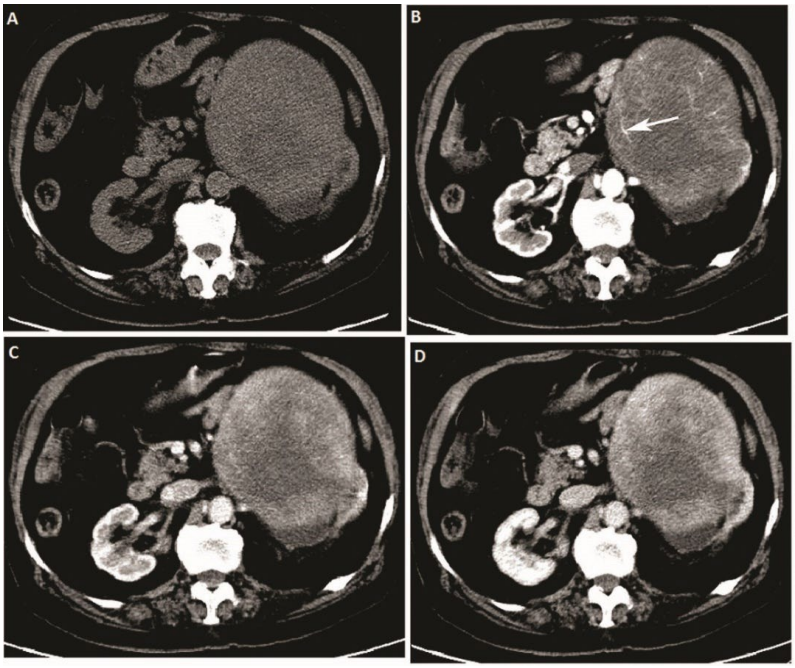

Figure 3: A 63 years old male with solitary fibrous tumor in left parotid gland extending to the para-pharyngeal space. A: The plain CT scan shows a homogeneous iso-dense mass with ill-defined margin; B: Marked heterogeneous enhancement is seen on arterial phase; C: Persistent enhancement is seen on venous phase; D: Histopathological analysis shows the hypercellular areas, composed of proliferation of spindle cells around with hyalinized collagen. Immune histochemical results are positive for CD34, bcl-2.

SFT, the serpentine vessels are often appeared in AP [21-23] which is defined as an important sign in SFT diagnosis. Fourteen cases presented vessel sign with linear and tortuous enhanced vessels along the periphery in this group. In our study, most tumors presented as a large heterogeneous tumor with myxomatous degeneration, which was slightly enhanced in arterial phase with prominent serpentine vessels inside (Figures 3 and 5).

MR has more advantages in reflecting the fibrous and collagenous component of SFT. They usually present homogeneous iso or hypo-intense signal on TIWI and heterogeneous iso or hyper-intense signal

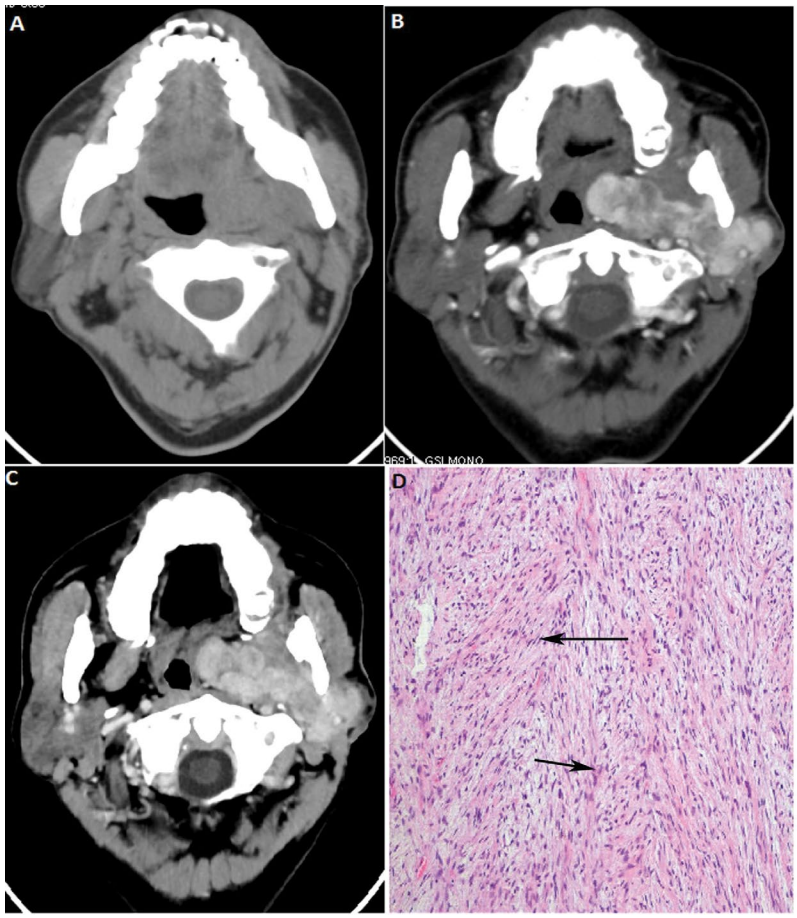

Figure 4: A giant solitary tumor in the left thoracic cavity of a 25 years old female. A: An oval homogeneous mass is seen on the plain CT scan, with a smooth and well-defined margin; B: After administration of contrast medium, the tumor is seen to be heterogeneously enhanced. Under the hypo-dense background, vessels are standing out predominantly; C: Pathological features shows hypo-cellular areas composed of rare spindle cells (arrow) and D: abundant collagenous stroma, mixed with haphazard ectatic vessels (arrow).

Figure 5: SFT of left kidney in a 77 years old female. A: The plain CT scan shows an oval heterogeneous mass in the left kidney; B: Slight heterogeneous enhancement is presented on arterial phase, with enhanced linear vessels along the lesion periphery (arrow); C and D: Progressive enhancement is seen on portal and venous phases. A patchy area of necrosis is seen to occur (arrow).

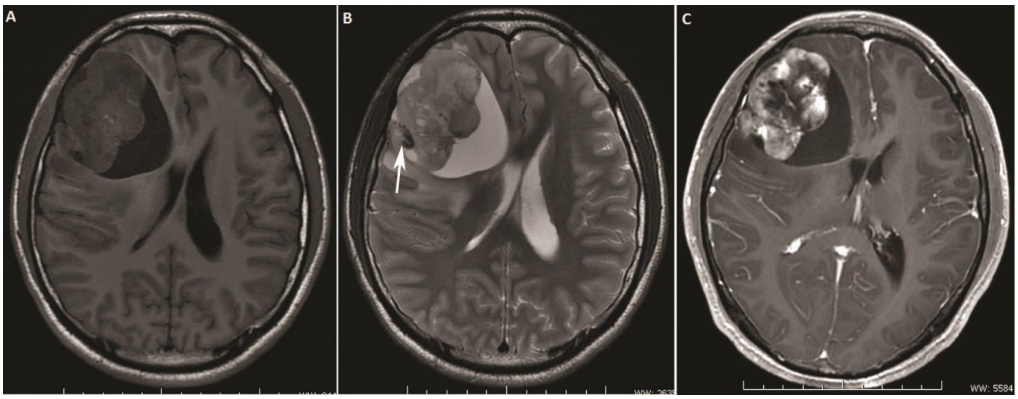

Figure 6: 26 year's old male with solitary fibrous tumor in the right frontal meanings. A: An iso- and hypo-intense signal is presented in the right frontal lobe on T1WI; B: T2WI exhibits a "black-and-white" mixed pattern from the mixed-intense signal with crescent cystic change. Serpentine vessels appeared as flow voids can be observed clearly (arrow); C: Heterogeneous enhancement indicates the hyper-vascular feature of tumor, which was misdiagnosed as schwannoma initially.

on T2WI. Hyper-intensity on T2WI is related to necrotic or cystic changes and myxomatous degeneration [17,24]. One case occurred in frontal lobe meninges in this study presented as a mixed signal mass with crescent hyper-intense area (Figure 6), which is called a "black-and-white" mixed pattern or "yin-yang" pattern in reported literature [25]. After gadolinium administration, small SFT usually presents homogeneous marked enhancement, while heterogeneous enhancement on large lesions. Due to the rich content of fibers and collagenous stroma, progressive enhancement is exhibited on dynamic contrast enhanced images [17]. Flow voids sign on T2WI is an important diagnostic clue to SFT (4, Error! Bookmark not defined. Error! Bookmark not defined. Error! Bookmark not defined.), which reveals the hyper-vascular feature of SFT like serpentine vessel sign on enhanced CT images. The majority (6/7) of our cases showed flow voids sign except the smallest lesion in the cervical spinal canal. Although most extra-pleural SFTs have been reported to be benign histologically, approximately 10% ~ 15% of tumors express malignant behavior in the form of recurrence or metastasis [24]. General histological features that may add clue to identify malignant lesion includes large size, infiltrative margin, hyper-cellularity, nuclear atypia, mitotic activity (≥ 4/10 high power fields) and the presence of necrosis and hemorrhage [13,24]. In our cases 17 were proven as benign, 4 border-line and 7 malignant in the final pathological result. Although large necrosis or cystic degeneration was reported in previous study might prompt suspicious for a malignant tumor, no significant correlation was found in this study. Ill-defined margin, invasion to adjacent tissues and indirect sign such as pleural effusion are the exceptional findings to suggest malignant nature in our cases. Of the 9 cases that had positive infiltrative manifestations, 4 cases were proven malignant and 2 borderline malignant. In addition, out of the 4 lesions that occurred in the mediastinum, 2 lesions were malignant and 2 were borderline nature. One of them experienced local recurrence one year after surgery, so it might prompt that tumors occurred in the mediastinum are more inclined to be malignant and need frequent follow-up after surgery.

SFTs are commonly misdiagnosed due to the rarity and lack of experience. Differential diagnosis can range from a broad spectrum of spindle-cell tumors to other hyper-vascular tumors (Error! Bookmark not defined. Error! Bookmark not defined) [26]. Seen from our results, most SFTs in thoracic cavity were diagnosed as sarcoma and mesothelioma initially because of the large size and hyper-vascularity. Extra-pleural SFTs can be misdiagnosed diversely, such as schwannoma and lung cancer in the mediastinum, meningioma and angio-fibroma in the head and neck region, hemangioma, hemangiopericytoma and stromal tumor in the abdominal cavity.

Conclusion

SFT usually appears as a slow-growing asymptomatic mass which can occur in various extra-pleural regions not only in pleura. Imaging findings typically reveal a large well-defined hyper-vascular tumor, some with variable degree of necrosis and cystic change. Two enhancement patterns can be present: marked and persistent enhancement, slight and progressive enhancement on the dynamic contrasted scanning. MRI images show homogeneous iso or hypo-intense signal on TIWI, and heterogeneous iso or hyper-intense signal on T2WI. Serpentine vessels enhanced in arterial phase and flow voids sign on T2WI are important diagnostic features. Most of SFTs are benign, but tumors accompanied with infiltrative signs prompt the suspicion for borderline or malignant nature and close long-term follow-up is recommended after surgery.

References

1. Klemperer P, Rabin CB (1931) Primary neoplasms of pleura: A report of five cases. Arch Pathol 11: 385-412.
2. Martin AJ, Fisher C, Igbaseimokumo U, Jarosz JM, Dean AF (2001) Solitary fibrous tumors of meninges: Case series and literature review. J Neurooncol 54: 57-69.
3. Kim HJ, Lee HK, Seo JJ (2005) MR imaging of solitary fibrous tumors in the head and neck. Korean J Radiol 6: 136-142.
4. Jeong AK, Lee HK, Kim SY, Cho KJ (2002) Solitary fibrous tumor of the parapharyngeal space: MR Imaging findings. Am J Neuroradiol 23: 473-475.
5. Chun HJ, Byun JY, Jung SE, Kim KH, Shinn KS (1998) Benign solitary fibrous tumor of the pre-sacral space: MRI findings. Br J Radiol 71: 677-679.
6. Fuksbrumer MS, Klimstra D, Panicek DM (2000) Solitary fibrous tumor of the liver: Imaging findings. AJR Am J Roentgenol 175: 1683-1687.
7. Moser T, Nogueira TS, Neuville A (2005) Delayed enhancement pattern in a localized fibrous tumor of the liver. AJR Am J Roentgenol 184: 1578-1580.
8. Nagasako Y, Misawa K, Kohashi S, Sano H (2004) Solitary fibrous tumor in the retroperitoneum. J Am Coll Surg 198: 322-323.
9. O'Connell JX, Logan PM, Beauchamp CP (1995) Solitary fibrous tumor of the periosteum. Hum Pathol 26: 460-462
10. Suster S, Nascimento AG, Miettinen M, Sickel JZ, Moran CA (1995) Solitary fibrous tumors of soft tissue: A clinicopathologic and immunohistochemical study of 12 cases. Am J Surg Pathol 19: 1257-1266.
11. Nielsen GP, O'Connell JX, Dickersin GR, Rosenberg AE (1997) Solitary fibrous tumor of soft tissue: A report of 15 cases, including 5 malignant examples with

light microscopic, immunohistochemical, and ultrastructural data. Mod Pathol 10: 1028-1037.

12. Guillou L, Fletcher JA, Fletcher CDM, Mandahl N (2002) Extrapleural solitary fibrous tumor and hemangiopericytoma. World Health Organization classification of tumours. Pathology and genetics of tumours of soft tissue and bone. Lyon: IARC Press, pp: 86-90.
13. Vallet-Decouvelaere AV, Dry SM, Fletcher CD (1998) Atypical and malignant solitary fibrous tumors in extrathoracic location: Evidence of their comparability to intra-thoracic tumors. Am J Surg Pathol 22: 1501-1511.
14. Abe S, Imamura T, Tateishi A (1999) Intramuscular solitary fibrous tumor: A clinicopathological case study. J Comput Assist Tomogr 23: 458-462.
15. Hasegawa T, Matsuno Y, Shimoda T, Hasegawa F, Sano T, et al. (1999) Extrathoracic solitary fibrous tumors: Their histological variability and potentially aggressive behavior. Hum Pathol 30: 1464-1473.
16. Yang BT, Wang YJ, Dong JY, Wang XY, Wang ZC (2012) MRI study of solitary fibrous tumor in the orbit. AJR Am J Roentgenol 199: W506-511.
17. Shanbhogue AK, Prasad SR, Takahashi N, Vikram R, Zaheer A (2011) Somatic and visceral solitary fibrous tumors in the abdomen and pelvis: Cross-sectional imaging spectrum. Radiographics 31: 393-408.
18. Zhang WD, Chen JY, Cao Y, Liu QY, Luo RG (2011) Computed tomography and magnetic resonance imaging findings of solitary fibrous tumors in the pelvis: Correlation with histopathological findings. Eur J Radiol 78: 65-70.
19. Rosenkrantz AB, Hindman N, Melamed J (2010) Imaging appearance of solitary fibrous tumor of the abdominopelvic cavity. J Comput Assist Tomogr 34: 201-205.
20. Rosado-de-Christenson ML, Abbott GF, McAdams HP, Franks TJ, Galvin JR (2003) From the archives of the AFIP: Localized fibrous tumor of the pleura. Radiographics 23: 759-783.
21. Soussan M, Felden A, Cyrta J, Morere JF, Douard R, et al. (2013) Solitary fibrous tumor of the liver. Radiology 269: 304-308.
22. Li XM, Reng J, Zhou P (2014) Solitary fibrous tumor in abdomen and pelvis: Imaging characteristics and radiologic-pathologic correlation. World J Gastroenterol 20: 5066-5073.
23. Tian TT, Wu JT, Hu XH (2014) Imaging findings of solitary fibrous tumor in the abdomen and pelvis. Abdom Imaging 39: 1323-1329.
24. Gengler C, Guillou L (2006) Solitary fibrous tumor and hemangiopericytoma: Evolution of concept. Histopathology 48: 63-74.
25. Wu YP, Huang B, Liang CH (2012) Solitary fibrous tumor of filum terminale. Acta Radiol Short Rep 1: 1-3.
26. Ganly I, Patel SG, Stambuk HE (2006) Solitary fibrous tumors of the head and neck: A clinicopathologic and radiologic review. Arch Otolaryngol Head Neck Surg 132: 517-525.